PHYSICAL REVIEW B **81**, 220503(R) (2010)

Incommensurate itinerant antiferromagnetic excitations and spin resonance in the $FeTe_{0.6}Se_{0.4}$ superconductor

D. N. Argyriou,[1,*] A. Hiess,[2] A. Akbari,[3] I. Eremin,[3,4,†] M. M. Korshunov,[3,5,‡] Jin Hu,[6] Bin Qian,[6] Zhiqiang Mao,[6] Yiming Qiu,[7,8] Collin Broholm,[9] and W. Bao[10,§]

[1]*Helmholtz-Zentrum Berlin für Materialen und Energy, Hahn Meitner Platz 1, D-14109 Berlin, Germany*
[2]*Institut Max von Laue-Paul Langevin, 6 rue Jules Horowitz, BP 156, F-38042 Grenoble Cedex 9, France*
[3]*Max-Planck-Institut für Physik komplexer Systeme, D-01187 Dresden, Germany*
[4]*Institute für Mathematische und Theoretische Physik, TU Braunschweig, D-38106 Braunschweig, Germany*
[5]*L.V. Kirensky Institute of Physics, Siberian Branch, Russian Academy of Sciences, 660036 Krasnoyarsk, Russia*
[6]*Department of Physics, Tulane University, New Orleans, Louisiana 70118, USA*
[7]*NIST Center for Neutron Research, National Institute of Standards and Technology, Gaithersburg, Maryland 20899, USA*
[8]*Department of Materials Science and Engineering, University of Maryland, College Park, Maryland 20742, USA*
[9]*Institute for Quantum Matter and Department of Physics and Astronomy, The Johns Hopkins University, Baltimore, Maryland 21218, USA*
[10]*Department of Physics, Renmin University of China, Beijing 100872, China*

(Received 10 May 2010; published 14 June 2010)

We report on inelastic neutron-scattering measurements that find itinerantlike incommensurate magnetic excitations in the normal state of superconducting $FeTe_{0.6}Se_{0.4}$ ($T_c=14$ K) at wave vector $\mathbf{Q}_{inc}=(1/2\pm\epsilon,1/2\mp\epsilon)$ with $\epsilon=0.09(1)$. In the superconducting state only the lower energy part of the spectrum shows significant changes by the formation of a gap and a magnetic resonance that follows the dispersion of the normal-state excitations. We use a four band model to describe the Fermi-surface topology of this iron-based superconductors with the extended $s(\pm)$ symmetry and find that it qualitatively captures the salient features of these data.

DOI: 10.1103/PhysRevB.81.220503 PACS number(s): 74.70.Xa, 74.20.−z, 78.70.Nx

Magnetism is a key ingredient in the formation of Cooper pairs in unconventional high-temperature superconductors.[1] A consequence of magnetism and the symmetry of the superconducting order parameter is a magnetic resonance that has been detected through inelastic neutron scattering for a wide range of magnetic superconductors ranging from the heavy fermion systems,[2] to cuprates,[3] and more recently in the iron-based superconductors.[4–6] In each class of materials the features of the resonance in $\mathbf{S}(\mathbf{Q},\omega)$ are different and are directly related to the electronic degrees of freedom, providing vital clues to the role of magnetic fluctuations in each case. We report inelastic neutron-scattering (INS) measurements showing that the magnetic excitations in $FeTe_{0.6}Se_{0.4}$ are incommensurate and itinerantlike, and that upon entering the superconducting state only the lower energy part of the spectrum shows significant changes by the formation of a gap and a magnetic resonance that follows the dispersion of the normal-state excitations. Using a four-band model that describes the Fermi-surface topology of iron-based superconductors and the extended $s(\pm)$ symmetry, we can qualitatively describe the salient features of the data.

In cuprate superconductors a magnetic resonance, whose energy scales with the superconducting energy gap, is a saddle point of a broader spectrum of magnetic excitations.[3,7] The interpretation of the magnetic resonance and its relationship to superconductivity is complicated in the cuprates due to the occurrence of charge stripes and the pseudogap phase that lead to hotly debated models such as quantum excitations from charge stripes[7] or spin excitons from a particle-hole bound state of a d-wave superconductor.[8–10]

A simpler picture has emerged in the iron-based superconductors partly due to their more itinerant nature. It was realized early on that the nesting between hole and electron Fermi surfaces related by the antiferromagnetic wave vector $\mathbf{Q}_{AF}=(\pi,\pi)$ in the undoped iron superconductors might also be responsible for unconventional superconductivity of the so-called extended $s(\pm)$-wave symmetry.[11–15] The remarkable feature of this superconducting order parameter is the different sign of the superconducting gap on bands that are separated by $\mathbf{Q}_{AF}$ can yield a magnetic resonance in the form of a spin exciton[16–24] at the same wave vector.

This picture suggests that the continuum of magnetic excitations will be gapped in the superconducting state up to twice the energy of the superconducting gap, 2Δ and that an additional feature, the magnetic resonance will occur at an energy $\hbar\omega_{res}<2\Delta$. The latter is a consequence of both the unconventional symmetry of the superconducting order parameter which enhances the continuum at 2Δ, and the residual interaction between the quasiparticles that shifts the pole in the total susceptibility to lower energies. While so far the magnetic resonance has been observed in iron-based superconductors at commensurate wave vectors, the itinerant origin of the magnetic fluctuations suggests that in the doped superconducting compounds, the nesting could be incommensurate.

In order to understand the extended magnetic excitation spectrum in iron-based superconductors we have chosen to examine the doped binary superconductor $FeTe_{0.6}Se_{0.4}$ with a superconducting $T_c=14$ K (see Fig. 3 in the supplementary information[25]), using INS. $FeTe_{0.6}Se_{0.4}$ crystallize in a primitive tetragonal structure $P4/mmn$, with $a=3.80$ Å and $c=6.02$ Å. A 2 g high quality single-crystal sample of this composition was prepared as described previously[26] and was part of a mosaic used in work described in Ref. 6. INS mea-

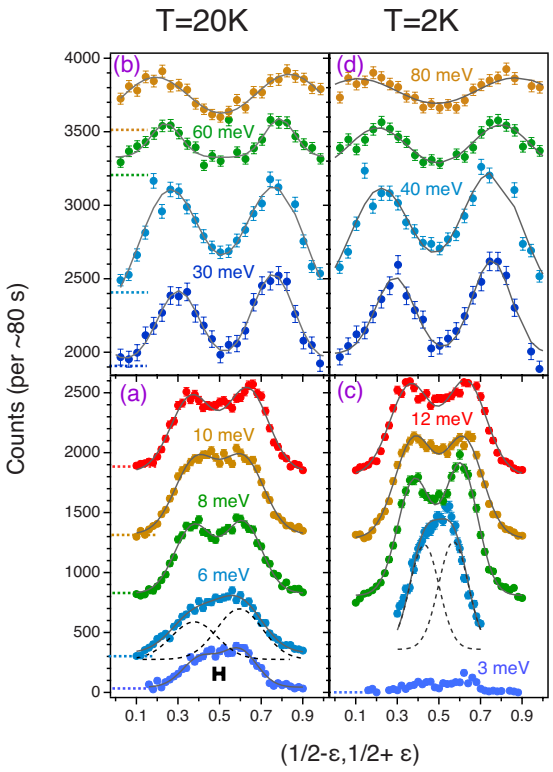

FIG. 1. (Color online) Typical INS transverse scans through $\mathbf{Q}=(1/2,1/2)$ at fixed $\hbar\omega$ measured from a single crystal of $FeTe_{0.6}Se_{0.4}$ at [(a) and (b)] 2 K below T_c and [(c) and (d)] at 20 K above T_c. The solid lines through the data are Gaussian fits to the magnetic excitations. For clarity, data and fits are shifted along the y axis by an arbitrary amounts. The position of the background for each scan is indicated by a horizontal line. The black horizontal bar in panel (a) represent the expected Q resolution.

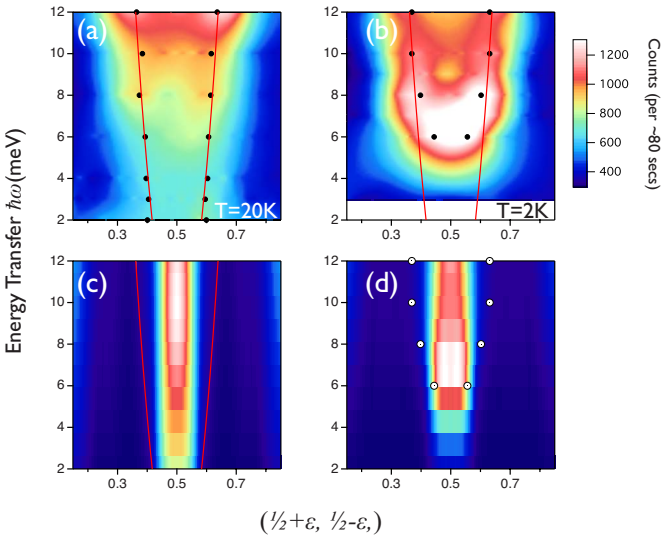

FIG. 2. (Color online) Color maps of the transverse fixed energy scans along $(1/2+\epsilon,1/2-\epsilon,0)$ for energy transfers between 2 and 12 meV measured at (a) 20 K and (b) 2 K. Black points indicate the center of Gaussian peaks fitted to the experimental data while the red lines illustrate the dispersions of these peak centers. In (b) black points represent centers of Gaussian from the subtraction shown in Fig. 3(b). The dispersion of the normal state is reproduced by red lines in the superconducting state to illustrate that the higher energy excitations have not changed their position below T_c. RPA calculations depicting the magnetic excitations of the (c) normal and (d) superconducting state. In (c) we over plot the experimental paramagnon dispersion while in (d) we show the measured magnetic-resonance excitations as white circles. The RPA calculations shown here were convoluted with a Gaussian instrument resolution function using an elastic energy resolution of $\Delta E=1$ meV and a transverse Q resolution of $\Delta Q\sim 0.06$ Å^{-1}.

surements were collected using the triple axis spectrometer IN8 operated by the Institut Laue-Langevin, with the sample mounted with the c-axis vertical giving us access to spin excitations within the basal ab plane. The neutron optics were set to focus on a virtual source of 30 mm. Measurements were made with the (002) reflection of a pyrolytic graphite monochromator and analyzer with an open/open/open/open configuration. A graphite filter was placed after the sample in the scattered beam to suppress second-order contamination while diaphragms were placed before and after the sample in order to minimize the background. Cooling of the sample was achieved by a standard orange cryostat. Data were collected around the (1/2,1/2,0) and (3/2,3/2,0) Brillouin zones using a fixed final wave vector k_f of either 2.66 or 4.1 Å^{-1} corresponding to an (elastic energy resolution) of 1 meV and 3.5 meV, respectively. In this work we describe the measurements in momentum space in units of $Q=(\pi/a,\pi/a)$ while we omit reference to the c-axis direction for clarity as $Q_z=0$ throughout. Background levels were established by scans away from the magnetic excitations between 2 and 80 meV and are shown in Fig. 1. Special care was given for 6 meV scan where the background was estimated to be approximately 360 counts per 80 s.

In the normal state we find steeply dispersive magnetic excitations that we have measured up to 80 meV, Figs. 1(a) and 1(b). At higher energies, two excitations are clearly resolved in the transverse scans. At lower energies (2–6 meV), the two peaks merge to a broad response and are best modeled by two broad peaks as illustrated for 6 meV data in Figs. 1(a) and 1(c).[27] At any energy transfer this peak width significantly exceeds the instrumental Q resolution, which has been experimentally verified for the elastic position and $k_f=2.662$ Å^{-1} on the (2 0 0) Bragg peak exhibiting a transverse Q width of $\Delta Q\sim 0.06$ Å^{-1}. In Fig. 2(a) we show the lower portion of these transverse scans in the normal state as a color map where in addition we plot as black points the $\mathbf{Q}$ position of the excitations determined by fitting Gaussian peaks to the data of Fig. 1. The dispersion of these excitations is linear up to 80 meV as shown in Fig. 3(a)and the points for the lower energy excitations fall on the same line confirming our above analysis. Extrapolating the centers of these excitations to zero energy, vertical red lines in Fig. 2(a), it is clear that they do not converge to the commensurate $\mathbf{Q}=(1/2,1/2)$ wave vector but to the incommensurate positions of $\mathbf{Q}_{inc}=(1/2\pm\epsilon,1/2\mp\epsilon)$ with $\epsilon=0.09(1)$. Excitations emanating from $\mathbf{Q}_{inc}=(1/2\pm\epsilon,1/2\pm\epsilon)$ were not observed consistent with Ref. 29. We note that for the FeTe end compound with lower excess Fe, static antiferromagnetism appears at $Q=(1/2,0)$.[28]

Longitudinal scans (not shown) between 2 and 80 meV

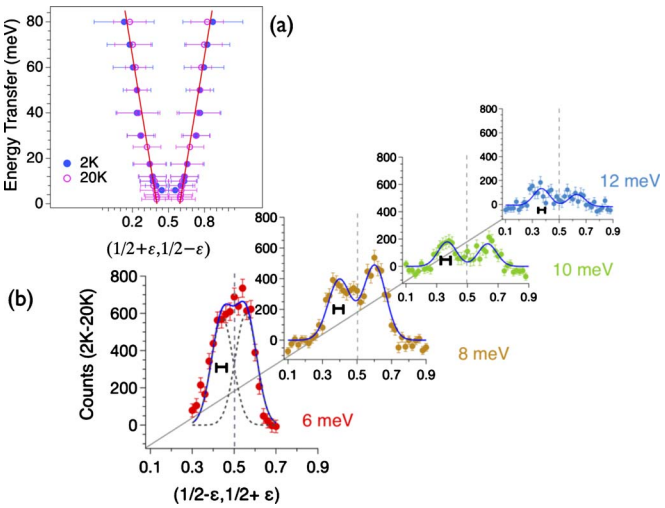

FIG. 3. (Color online) (a) Experimental dispersions of the magnetic excitations of $FeTe_{0.6}Se_{0.4}$ at 20 and 2 K determined by fitting Gaussian peaks to the measured excitations. A linear fit to the 20 K data is illustrated as a red lines. The horizontal errors bars indicate the full width at half maximum of the excitation determined from a fit of a Gaussian to the data. (b) Dispersion of the incommensurate spin resonance as determined from difference transverse INS scans through $\mathbf{Q}=(1/2,1/2)$ at various energy transfers between 6 and 12 meV. The difference is modeled using two Gaussians centered on incommensurate positions and the fit is shown as a continuous line through the data. For 6 meV data we shown the two individual peaks as dashed lines.

through these spin excitations show that they are well-defined isolated maxima and not parts of spin-wave cones as found in insulators, a conclusion concurred also in other recent INS measurements.[29] Therefore, we argue that magnetic excitations in the normal state of the superconductor $FeTe_{0.6}Se_{0.4}$ consists of a single excitation branch emerging from *each* incommensurate $\mathbf{Q}_{inc}$. This behavior in $S(\mathbf{Q},\omega)$ is reminiscent of Fincher-Burke excitations reported for many itinerant magnetic materials that are close to an antiferromagnetic instability[30–33] and indicates that an itinerant, rather than a local-moment picture is relevant for this superconductor.

Cooling below T_c we find substantial changes to the lower energy magnetic excitations while our measurements indicate that the higher energy excitations remain largely unchanged when compared to the normal-state measurements, see Figs. 1(b) and 1(d). We also note that the compositional dependence of these higher energy excitations appears also to be weak as shown in Ref. 29. The most pronounced changes are in the lower energy part of the magnetic excitation spectrum where the opening of a spin gap and the development of the magnetic resonance is observed as shown in Fig. 2(b). Here a spin gap opens below $\hbar\omega=4$ meV while there is an enhancement of the spectral weight above the spin gap that peaks at $\hbar\omega_{res}=6$ meV. At higher energies the spectral weight returns to approximately the same values as the data found in the normal state, see Fig. 1. Constant energy scans at the commensurate position $\mathbf{Q}=(1/2,1/2)$ between these dispersions also reflect these changes as shown in Ref. 6. Analysis of the data shown in Fig. 1, as well as energy scans measured at $\mathbf{Q}=(1/2,1/2)$ (not shown) indicate that the temperature-independent sum rule for neutron magnetic scattering $\int d\omega \int d\mathbf{Q} S(\mathbf{Q},\omega)$, holds above and below T_c within 2% of the total counts.

Although the normal-state magnetic excitations extend from incommensurate points it is important to establish if the magnetic resonance itself is centered on the commensurate wave vector $\mathbf{Q}=(1/2,1/2)$ or if it consists of two excitations originating from the two incommensurate wave vectors (at $\mathbf{Q}_{inc}$) found in the normal state. For a more detailed analysis of the Q scans across the resonance we subtract the 20 K from the 2 K data in order to obtain only the magnetic scattering contributing to the resonance (see below). These data are shown in Fig. 3(b) while the centers of the resonant excitations are plotted in Fig. 2(b). Between $\hbar\omega=7$ and 12 meV, the data show well separated resonant excitations that follow the normal-state dispersions while their intensity decreases with energy transfer giving only a minor superconducting enhancement at 12 meV. At the resonance, however, $\hbar\omega_{res}=6$ meV, a "flat top" excitation is evident that can be modeled with two incommensurate peaks at $\mathbf{Q}_{res}=(\frac{1}{2}\pm\epsilon,\frac{1}{2}\mp\epsilon)$ with $\epsilon=0.05(1)$, a value that departs slightly from the one found in the normal state.

Our INS results are qualitatively consistent with the extended $s(\pm)$ model of the superconducting order parameter as we indeed observe the opening of a spin gap and the enhanced peak just above the gap as expected. However it is less clear if the magnetic resonance and its spectral weight in $S(\mathbf{Q},\omega)$ is consistent with this model. To clarify this we compute the magnetic susceptibility within this four-band model[22] and use the conventional random-phase approximation (RPA) which describes the enhancement of the spin response of a metal. In Figs. 2(c) and 2(d) we show the results for the total *physical* RPA susceptibility, $\chi_{\mathrm{RPA}}(\mathbf{q},i\omega_m)=\sum_{i,j}\chi^{i,j}_{\mathrm{RPA}}(\mathbf{q},i\omega_m)$, calculated for the Fermi-surface topology that is consistent with ARPES (angle resolved photoemission spectroscopy) results on $Fe_{1.03}Te_{0.7}Se_{0.3}$ (Ref. 34) as a function of the momentum along the transverse direction $(1/2+\epsilon,1/2-\epsilon)$ and $\hbar\omega$ in the normal and superconducting states (details of these calculations are presented in the supplementary information). Due to the nesting condition[35] of one of the hole bands (α) and the two electron bands (β) (see Fig. 1 in the supplementary information) we find that in the normal state the spin response shows antiferromagnetic excitations centered on an incommensurate transverse wave vector with $\epsilon=0.03$. These low-energy magnetic excitations in the metals, often called *paramagnons*, result from the proximity of the Fermi surface to a magnetic instability and in our model we find that they disperse linearly from the incommensurate wave vectors. While the RPA theory indicates two peaks for each incommensurate wave vector (counter propagating linearly dispersive modes), only a single peak is observed experimentally dispersing from each $\mathbf{Q}_{inc}$ wave vector, suggesting stronger electronic damping than the current RPA treatment, as demonstrated previously by Moriya and Ueda.[36]

In the superconducting state, the magnetic susceptibility changes due to opening of the superconducting gap and the corresponding change in the quasiparticle excitations, affecting directly the lower energy excitations while leaving the

higher energy part of the spectrum unchanged in our agreement with our measurements. Here the imaginary part of the bare interband susceptibility (i.e., without electron-electron interaction that yields RPA) is gapped for small frequencies and at the antiferromagnetic wave vector $\mathbf{Q}_{AF}$, the value of this gap is determined as $\Omega_c=\min(|\Delta_{\mathbf{k}}|+|\Delta_{\mathbf{k}+\mathbf{Q}_{AF}}|)\sim 2\Delta_0 \sim 8$ meV (Ref. 34), where Δ_0 is the superconducting gap. Furthermore, above Ω_c the imaginary part of the bare interband susceptibility shows the discontinuous jump implied by the Bogolyubov coherence factor $(1+\frac{\Delta_{\mathbf{k}}\Delta_{\mathbf{k}+\mathbf{Q}_{AF}}}{|\Delta_{\mathbf{k}}||\Delta_{\mathbf{k}+\mathbf{Q}_{AF}}|})$ and the condition $\Delta_{\mathbf{k}}=-\Delta_{\mathbf{k}+\mathbf{Q}_{AF}}$. The latter is true for the $s\pm$-wave symmetry of the superconducting order parameter. Correspondingly, the real part of the bare susceptibility is positive, diverges logarithmically at $\Omega_c=2\Delta_0$, and scales as ω^2 at small frequencies.[22] Then, switching on the electron-electron interactions, we find within RPA that for any positive value of the interband interaction the total (RPA) spin susceptibility acquires a pole or *spin exciton* below Ω_c with infinitely small damping. Therefore, other than the gapping of the spin spectrum, the most salient point of our analysis is that it predicts a spin exciton at $\hbar\omega_{res}\approx 6$ meV in the superconducting state that is located at the same incommensurate wave vectors as paramagnons in the normal state, a feature that is clearly found in our INS data. We stress here that the spin exciton is a property of the superconducting state and requires opposite sign of the superconducting order at the corresponding wave vector, i.e., $\Delta_{\mathbf{k}}=-\Delta_{\mathbf{k}+Q_{AF}}$. We remark that the actual spin gap in the neutron spectrum is smaller than $2\Delta_0$ which is again a consequence of the spin exciton formation in the superconducting state.

Our itinerant RPA like description is obviously not sufficiently accurate to describe all the detailed features of the spin excitation spectrum. For example, the dispersion of the paramagnons are steeper than observed as shown in Fig. 2(c) while the value for the incommensurability ϵ is smaller than the experimentally observed, although better agreement can be obtained if the ellipticity of the electron pocket at the M point is considered.[37] Nevertheless, our treatment captures the key points of the data, these being the incommensurate paramagnon excitations, the emergence of the spin gap and the superposition of the exciton in the superconducting state onto the paramagnon scattering.

To summarize, we find using inelastic neutron scattering that in the $FeTe_{0.6}Se_{0.4}$ superconductor the magnetic resonance appears superimposed at the incommensurate wave vector as paramagnon excitations found in the normal state. Our simple RPA model of the magnetic excitations on the basis of the $s(\pm)$ symmetry of the superconducting order parameters can qualitatively reproduce the main features of the neutron-scattering data. The agreement supports an itinerant character of the spin excitations in iron-based systems and a spin spectrum determined by the single poles of Im χ with no extra contributions from localized moments.

Work at Tulane was supported by the NSF under Grant No. DMR-0645305 (for materials) and the DOE under Grant No. DE-FG02-07ER46358 (for graduate students). Work at JHU was funded by the DOE under Grant No. DE-FG02-08ER46544. D.N.A. benefited from helpful discussions with Jan Zaanen and Alan Goldman and thanks the DFG for support under SPP 1458. M.M.K. is grateful to P. J. Hirschfeld for useful discussions and acknowledges support from RFBR (Grant No. 09-02-00127), OFN RAS program on strong electronic correlations, and the Russian FCP (Grant No. NK-589P/46).

*argyriou@helmholtz-berlin.de

†ieremin@mpipks-dresden.mpg.de

‡Present address: Department of Physics, University of Florida, Gainesville, Florida 32611, USA.

§wbao@ruc.edu.cn

[1] A. Chubukov *et al.*, *Superconductivity* (Springer-Verlag, Berlin, 2008), Vol. 2, p. 1349.

[2] A. Hiess *et al.*, J. Phys.: Condens. Matter **18**, R437 (2006), topical review.

[3] Ph. Bourges *et al.*, Physica C **424**, 45 (2005).

[4] A. D. Christianson *et al.*, Nature (London) **456**, 930 (2008).

[5] M. D. Lumsden *et al.*, Phys. Rev. Lett. **102**, 107005 (2009).

[6] Y. Qiu *et al.*, Phys. Rev. Lett. **103**, 067008 (2009).

[7] J. M. Tranquada *et al.*, Nature (London) **429**, 534 (2004).

[8] K. Maki *et al.*, Phys. Rev. Lett. **72**, 1758 (1994).

[9] P. Monthoux *et al.*, Phys. Rev. Lett. **72**, 1874 (1994).

[10] J.-P. Ismer *et al.*, Phys. Rev. Lett. **99**, 047005 (2007).

[11] I. I. Mazin *et al.*, Phys. Rev. Lett. **75**, 4134 (1995).

[12] I. I. Mazin *et al.*, Phys. Rev. Lett. **101**, 057003 (2008).

[13] A. V. Chubukov *et al.*, Phys. Rev. Lett. **101**, 147004 (2008).

[14] A. V. Chubukov *et al.*, Phys. Rev. B **78**, 134512 (2008).

[15] S. Graser *et al.*, New J. Phys. **11**, 025016 (2009).

[16] A. Abanov *et al.*, Phys. Rev. Lett. **83**, 1652 (1999).

[17] J. Brinckmann *et al.*, Phys. Rev. Lett. **82**, 2915 (1999).

[18] Y.-J. Kao *et al.*, Phys. Rev. B **61**, R11898 (2000).

[19] D. Manske *et al.*, Phys. Rev. B **63**, 054517 (2001).

[20] M. R. Norman, Phys. Rev. B **61**, 14751 (2000).

[21] A. V. Chubukov *et al.*, Phys. Rev. B **63**, 180507(R) (2001).

[22] M. M. Korshunov *et al.*, Phys. Rev. B **78**, 140509(R) (2008).

[23] K. Seo *et al.*, Phys. Rev. B **79**, 235207 (2009).

[24] T. A. Maier *et al.*, Phys. Rev. B **79**, 134520 (2009).

[25] See supplementary material at http://link.aps.org/supplemental/10.1103/PhysRevB.81.220503 for the magnetic susceptibility of our sample.

[26] T. J. Liu *et al.*, Phys. Rev. B **80**, 174509 (2009).

[27] Special care was given for 6 meV scan where the background was estimated to be approximately 360 counts per 80 s.

[28] W. Bao *et al.*, Phys. Rev. Lett. **102**, 247001 (2009).

[29] M. D. Lumsden *et al.*, Nat. Phys. **6**, 182 (2010).

[30] E. Fawcett, Rev. Mod. Phys. **60**, 209 (1988).

[31] W. Bao *et al.*, Phys. Rev. B **54**, R3726 (1996).

[32] W. Bao *et al.*, Phys. Rev. B **76**, 180406(R) (2007).

[33] H. Kadowaki *et al.*, Phys. Rev. Lett. **101**, 096406 (2008).

[34] K. Nakayama *et al.*, arXiv:0907.0763 (unpublished).

[35] That is, $\varepsilon^{\alpha}_{\mathbf{k}}=-\varepsilon^{\beta}_{\mathbf{k}+\mathbf{Q}_{AF}}$.

[36] T. Moriya *et al.*, Rep. Prog. Phys. **66**, 1299 (2003).

[37] I. Eremin (private communication).